Applied Clay Science 246 (2023) 107190

Contents lists available at ScienceDirect

Applied Clay Science

journal homepage: www.elsevier.com/locate/clay

A particle-scale analysis of unload-reload hysteresis for normally consolidated kaolin

John de Bono , Glenn McDowell *

University of Nottingham, United Kingdom

ARTICLE INFO

Keywords:
Kaolinite
Modelling
Soil mechanics

ABSTRACT

The mechanical behaviour of sands and clays subject to "normal" (plastic) compression are very similar, albeit at different stress levels, despite the differences in inter-particle interactions (Hertzian normal contact forces or similar for sand) and electro-chemical forces for clays. However the hysteretic behaviour of clay is very different to sand with clays exhibiting "springy" hysteresis loops and ratchetting volumetric compaction. This paper aims to show that whereas the "plastic" compression arises from degradation of macro particles, the "quasi-elastic" unload-reload behaviour is consistent with an increase in the number of platelet edge contacts as clay "stacks" rearrange and compact.

1. Introduction

It is well-known that for normally consolidated clay, soils demonstrate hysteretic responses when unloaded and reloaded (e.g. Burland, 1990; Wood, 1990). In this paper, a particle-scale model was used to simulate the isotropic normal compression and unloading-reloading on a numerical sample of kaolin clay. Although both clays and sands share similar behaviour within the critical state soil mechanics framework, clays are unique in demonstrating well defined hysteretic loops during cyclic compression, with paths that are non-linear when plotted on semi-logarithmic volume-stress charts (Cui et al., 2013). The state-of-the-art model used here successfully captured this aspect of clay behaviour, and was used to analyse the particle-scale mechanisms that occur during unloading and reloading. The model was able to reveal some particle scale insights into the hysteresis.

2. Numerical model

2.1. Background

The particle-scale model is based on the discrete element method (DEM), and models kaolinite platelets using arrays of spheres. Much of this model is based on previous work by the authors (de Bono and McDowell, 2023a), and as such only key details will be repeated in this technical note. The platelets were constructed from two layers of spheres, as shown in Fig. 1(a). This is a convenient method of modelling the correct particle shape as well as achieving the desired surface interactions between the distinct faces of each platelet.

Kaolinite platelets were modelled with two distinct surfaces: a silica tetrahedral face and an alumina octahedral face (Mitchell and Soga, 2005). It was assumed that the silica face possesses a negative surface charge, and the alumina face a positive surface charge (Gupta and Miller, 2010; Liu et al., 2014b; Kumar et al., 2017). This corresponds to typical soil (and laboratory) conditions, with an acidic pH (≈5) and a moderate residual electrolyte content (Wang and Siu, 2006; Pedrotti and Tarantino, 2017). Earlier work by de Bono and McDowell (2022a, 2023b) explored varying the pH by adjusting the platelet interactions, and showed that for alkaline conditions (where all contacts are predominantly repulsive), denser samples were achieved, in agreement with experimental observations. Several attempts have been made in the past (e.g. Sjoblom, 2016; Pagano et al., 2020; Bandera et al., 2021) to perform particle-scale simulations of kaolin, and defining the interactions has remained an area of uncertainty.

2.2. Methodology

In this work, for simplicity it was assumed that opposite-charged kaolinite surfaces demonstrate long-range attraction, with stiff close-range repulsion; and that like-charged surfaces demonstrate monotonic repulsion. Although this is a simplification, it is advanced enough to capture all salient macroscopic features of clay behaviour (de Bono and McDowell, 2023a), and goes beyond previous studies which

* Corresponding author.
E-mail address: glenn.mcdowell@nottingham.ac.uk (G. McDowell).

https://doi.org/10.1016/j.clay.2023.107190
Received 18 August 2023; Received in revised form 23 October 2023; Accepted 24 October 2023

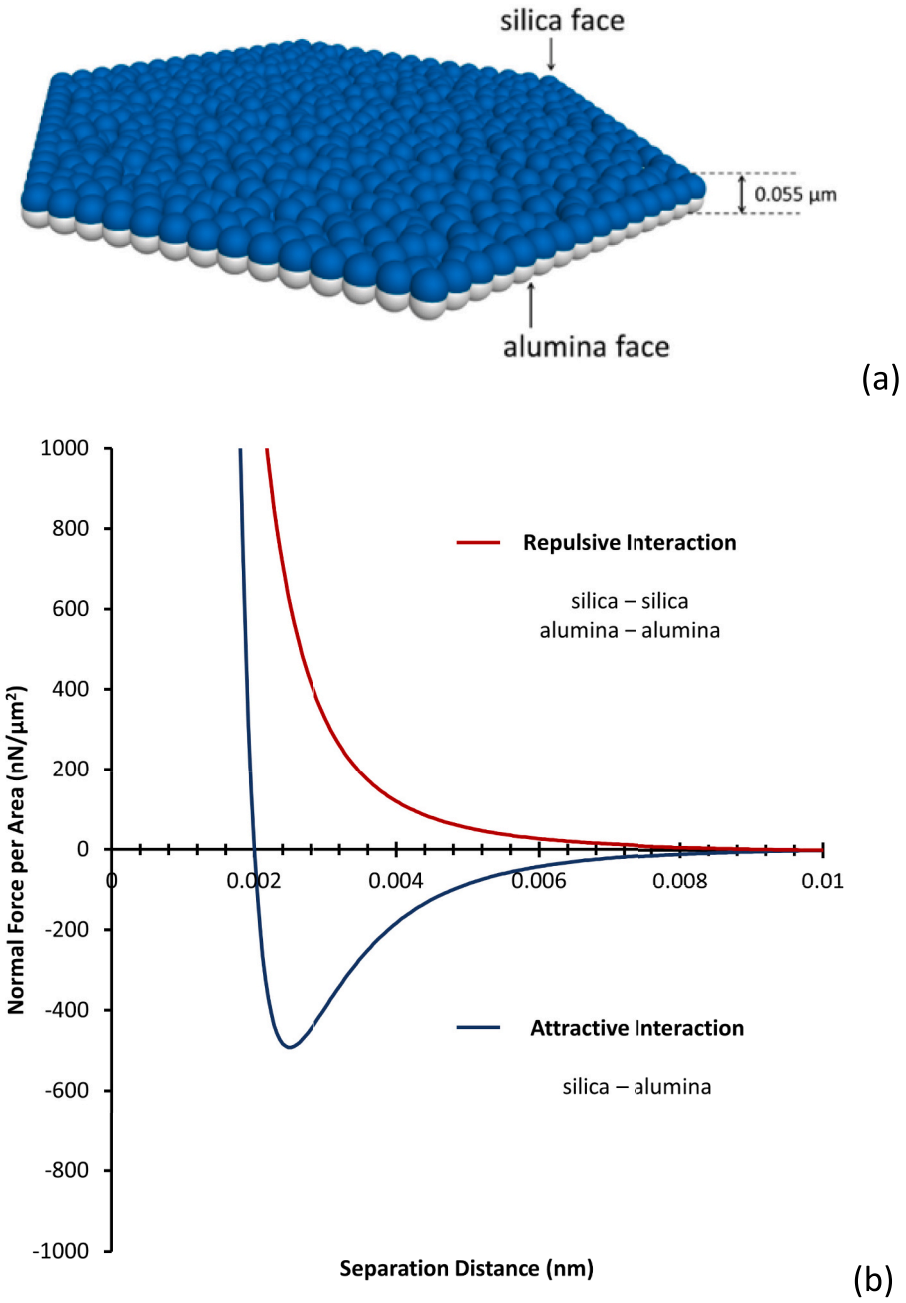

Fig. 1. (a) Platelets and (b) surface interactions.

typically did not differentiate between surfaces (e.g. Aminpour and Sjoblom, 2019) . In this model, the interactions (chiefly the pull-off forces) were estimated from various experimental surface force measurements. There are several Atomic Force Microscopy (AFM) studies probing the various kaolinite surfaces, and from these data it is possible to estimate equivalent interactions between flat surfaces using the Derjaguin approximation (Alcantar et al., 2003; Israelachvili, 2011). Based on AFM data (Veeramasuneni et al., 1996; Gupta and Miller, 2010; Liu et al., 2014a; Kumar et al., 2017), it was assumed here that the maximum pull-off force between the silica and alumina kaolinite surfaces is approximately 500 nN/µm^2. It was assumed that all interactions between surfaces have a cut-off range of 10 nm; this means that particles closer than this could be considered 'in contact' with each other, see de Bono and McDowell (2023a) for further details and justification. The interactions modelled are shown in Fig. 1(b)—and these are the inter-platelet interactions per unit area. To achieve these interactions, it was necessary to calibrate the sphere-to-sphere interactions, a simple and common procedure, outlined in de Bono and McDowell (2022b). The sphere-to-sphere interactions were very similar to the platelet interactions, but they are calibrated to ensure repeatability. For tangential interactions between platelets, a simple linear tangential stiffness (stiffness being the gradient of the force-displacement curve) with a limiting coefficient of friction was used. Like the normal interactions, choosing suitable tangential interactions involves a great deal of uncertainty; no direct measurements of forces have been made between kaolinite surfaces. In this work a coefficient of friction of 0.5 was applied for adhesive contacts, and a value of 0.05 was used for purely repulsive contacts; these values were chosen for simplicity, and based on relevant data available in the literature: friction coefficients of between 0.25 and 0.50 have been reported for sliding between adhesive mica or silica surfaces (Homola et al., 1989; Vigil et al., 1994; Kawai et al., 2015); and values of 0.02–0.05 for sliding between repulsive mica surfaces in

Table 1
Summary details of interactions between platelet surfaces.

Interacting Surfaces		Type	Pull-off Force (nN/μm^2)	Interaction Range (nm)	Friction Coefficient, μ
silica face	alumina face	*attractive*	500	10	0.50
silica face	silica face	*repulsive*	0	10	0.05
alumina face	alumina face	*repulsive*	0	10	0.05
silica face	boundary	*repulsive*	0	10	0.0
alumina face	boundary	*attractive*	500	10	0.0

aqueous solutions (Homola et al., 1990). De Bono and McDowell (2023a) found that universally low friction gives good normal compression behaviour but very low shear resistance. Universally high friction gives quasi-recoverable compression behaviour, which is not observed experimentally. By having high friction for attractive contacts and low friction for repulsive ones, much of the mechanical behaviour of kaolin can be reproduced. In summary, the interactions used in this model are shown in Fig. 1(b) and given in Table 1.

To create the initial sample, the platelets were created in 'stacks' (i.e aggregates of platelets). These stacks, shown in Fig. 2(a), can be considered as 'macro' particles, held together by the attraction between the opposite-charged kaolinite surfaces. Such stacks are invariably observed in SEM images of kaolinite slurries (e.g. Wang and Siu, 2006; Gupta et al., 2011; Pedrotti and Tarantino, 2017). Their use here not only resulted in realistic porosities following sedimentation of the sample, but also meant it was possible to fully explore the evolution of the macroparticle population as the stress was increased to levels seen in soils mechanics and foundation engineering. Although the sample simulated here assumed acidic conditions (pH ≈ 5), the observation of stacks from SEM also extends to alkaline conditions (where interactions are often assumed to be repulsive). It remains unclear whether stacks are formed/exist before or after sample preparation, but it is beyond doubt that they are always present in freshly prepared clay slurries. Although it is beyond the scope of this technical note, this is an active area of research, and the authors anticipate that to capture (or justify) the formation (or existence) of stacks in alkaline conditions, either an oscillatory interaction law or some heterogeneity in surface charges would be needed.

For simplicity, only a single stack arrangement was used, which was replicated several hundred times within a cylinder to create the whole sample. This sample was then compacted by applying a vertical stress of 100 kPa, to create a sample representative of a lightly consolidated clay slurry—shown in Fig. 2(b). This sample was the starting point for the compression simulation, which applied a (cyclic) isotropic stress. The initial sample contained 3234 platelets, in 462 stacks. The cylindrical boundary was modelled using a flexible faceted membrane, capable of applying a uniform pressure (de Bono and McDowell, 2023a). Each stack contained platelets with diameters of 1.5, 1.0 and 0.75 μm.

3. Results

The isotropic normal compression results are shown in Fig. 3, which includes three unload-reload loops. Although only a modest number of platelets were used, this simulation took several months to run, and involved computing the interactions between millions of spheres and applying small isotropic stress increments (10 kPa). It is clear that the behaviour is hysteretic, where permanent volumetric strain accrued with each cycle. The unloading and reloading lines are non linear when plotted on semi-logarithmic axes, which is in contrast to sands—both experimentally (e.g. Wood, 1990) and using DEM simulations (e.g. de

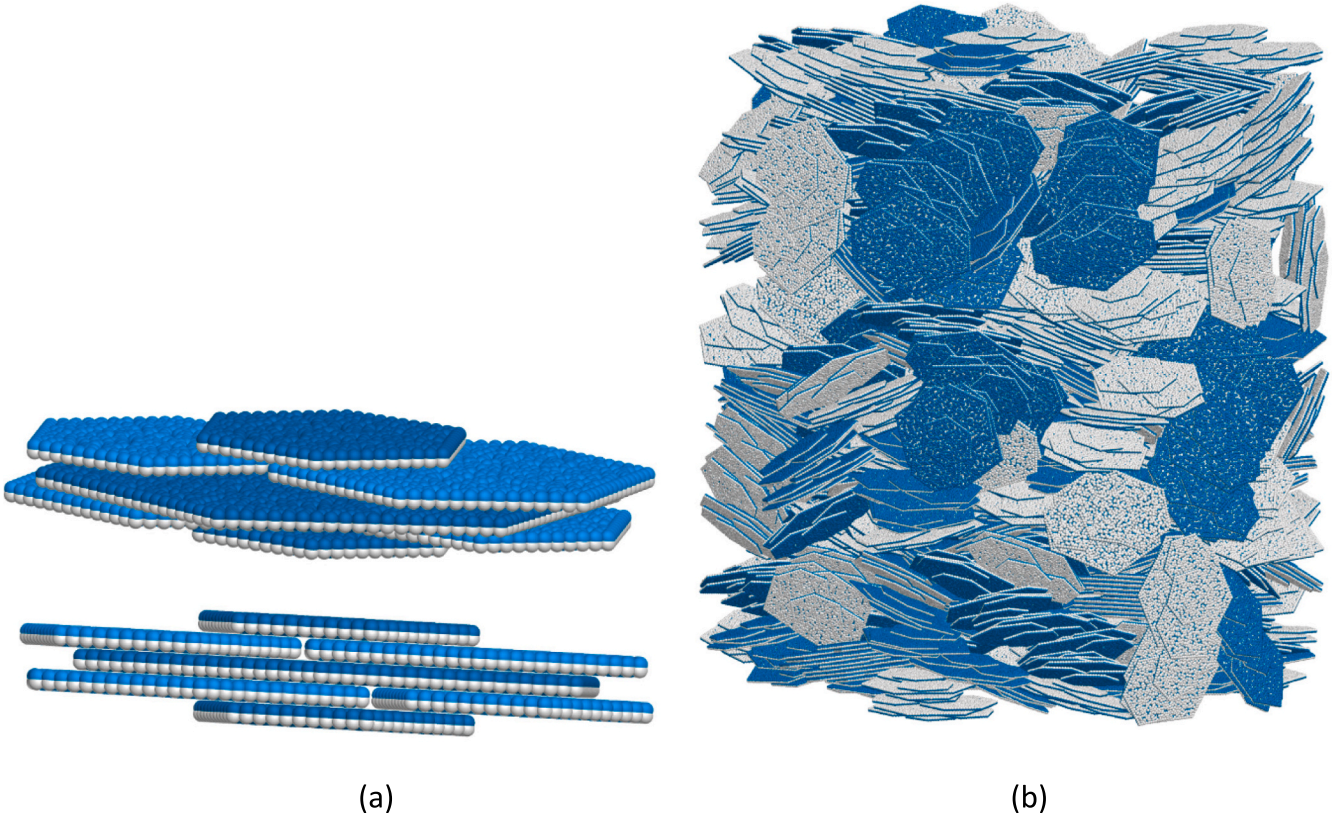

Fig. 2. Stacks of platelets (a), initial sample (b).

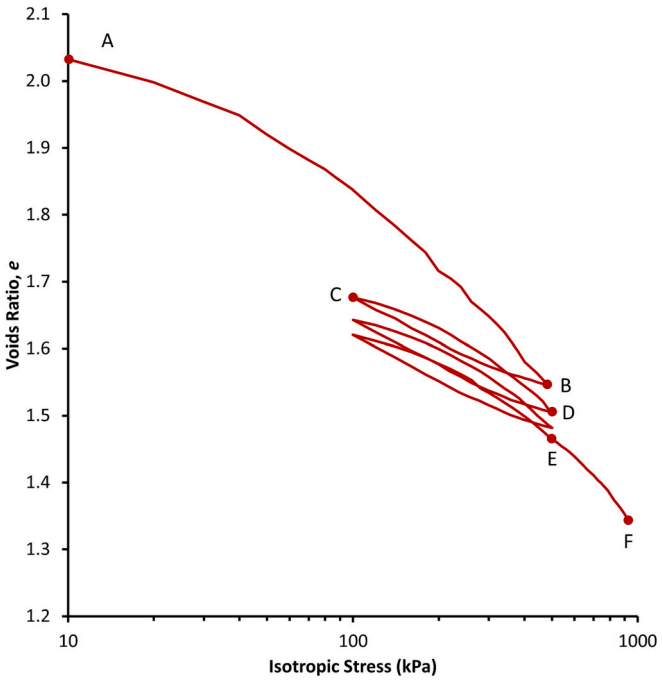

Fig. 3. Normal compression results including unload reload cycles.

Bono and McDowell, 2017). This behaviour occurred without any viscous damping imposed between the platelets, and resulted only from the platelets and their interactions. The key mechanisms during the "normal" (plastic) compression is the destruction/deformation of the aggregated particles (i.e. the stacks). This is demonstrated in Fig. 4(a), which shows the distribution of particle sizes at the start of the test (Point A), before and after reloading cycles (Points B, E), and after ultimate compression to 1000 kPa (Point G). Whilst significant changes occurred with increasing stress on the normal compression line from A to B to F, the unload-reload cycles had relatively little impact.

To investigate what occurred during compression and during the unload-reload loops, it was possible to analyse the type of interactions (or 'contacts') between the platelets. All interactions between platelets could be categorised as either 'Face-to-Face' or an 'Edge Contact'. Face-to-face contacts were those interactions between (approximately) parallel platelets. These interactions include platelets which are adhered together within a stack, as well as between platelets which are repelling each other and not part of a stack. Edge contacts refer to all contacts where at least one platelet was predominantly interacting with another via an edge. This includes pairs of platelets which were almost parallel, perpendicular, or in an 'edge-to-edge' arrangement. Fig. 4(b) plots the evolution of these contacts with the applied stress, and shows that there was a decrease in face-to-face interactions during compression, and an increase in all other contacts. The reduction in face-to-face contacts was largely caused by the degradation of the stacked, parallel platelets. It is interesting to observe that the number of face-to-face interactions demonstrated a closed loop during unload-reloading, whilst the number of other contacts demonstrated an increase. This both confirms the degradation of aggregated 'macro' particles, and also reveals that a key feature (or outcome) of permanent volume reduction was the creation of more contacts as the platelets are forced into a tighter packing—occurring both during normal compression and during the reloading when the sample compresses further.

Compared to bulky materials, such as sand, the non-linear shape of the unloading line for clay appears a result of the complex network of contacts. This network, resulting from both platelet shape and the interactions, consists of a range of contacts with varying mechanisms. Parallel platelets, when loaded axially are very stable, stiff and elastic; however they can be sheared apart. Other types of contacts, between non-parallel platelets can also experience frictional sliding but can also demonstrate elastic behaviour or collapse.

It is the change in the physical packing which leads to a permanent volume decrease during the unload-reload loops, and this can be observed via particle displacements shown in Fig. 5. Fig. 5(a) shows the *in-plane* platelet displacements, on a vertical plane through the centre of the sample, between points B and C (the first unloading). It is clear that the predominant direction of motion for platelets in this plot is upwards, although there was much less displacement of the platelets at the bottom of the sample (the sample is top driven and fixed at the base so displacements on average will be proportional to distance from the base). Fig. 5(b) shows the displacements on the same plane during reloading, and it reveals slightly more displacement in the inwards-horizontal direction. This is consistent with Fig. 5(c), which plots the platelet

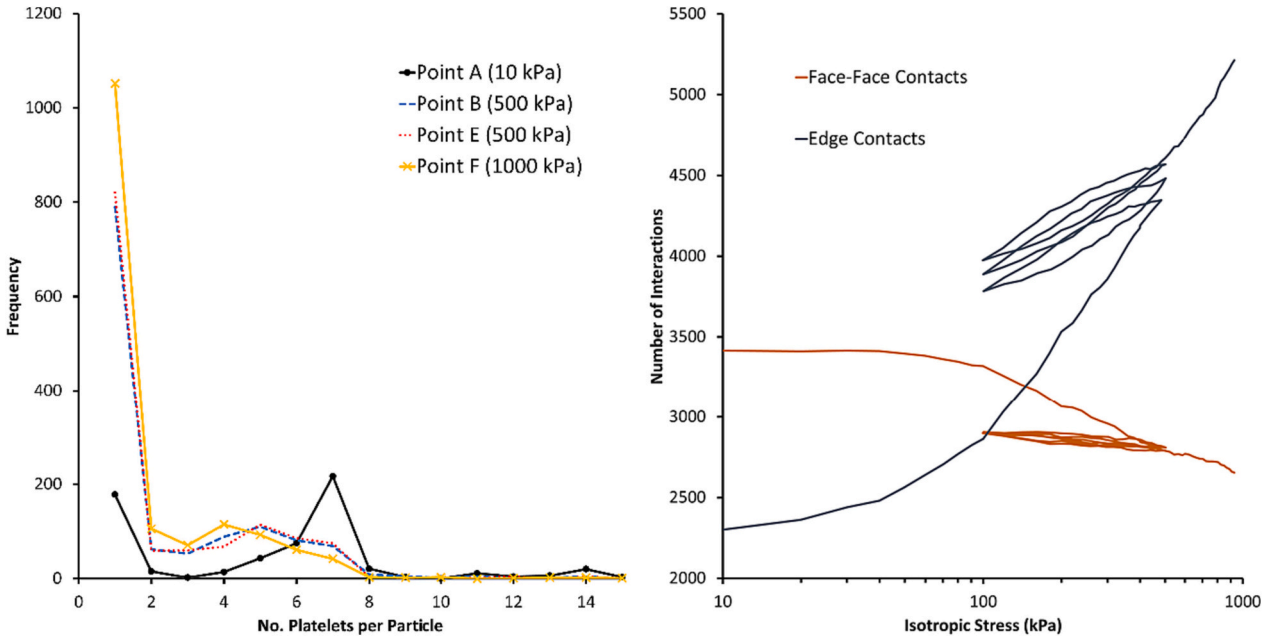

Fig. 4. (a) Size distribution of particles, and (b) evolution of different types of contacts.

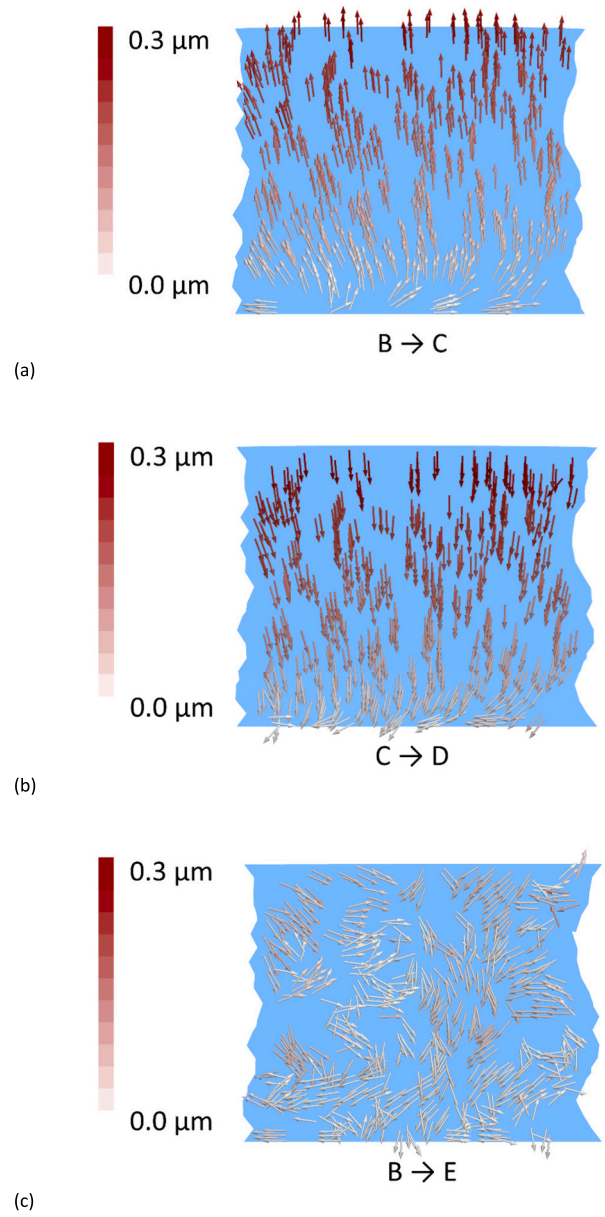

Fig. 5. Platelet displacements on a vertical plane through the sample.

displacements accrued during all unload-reload loops (point B to F). This plot shows that platelets have migrated mainly horizontally.

This finding is also confirmed in Fig. 6, which shows the various components of strain plotted during compression. During normal compression, the axial strain accrued more rapidly than the radial strain, meaning a resultant shear strain is applied (proportional to the difference), despite being loaded istropically, in a quasi-static manner. Interestingly, during cyclic loading, there is almost no overall change in axial strain, and the volumetric strain appears entirely attributable to the radial strain. There was very little 'rebound' in radial strain during unloading, and then permanent radial strain during reloading, which has the effect of 'undoing' some of the macroscopic shear strain.

4. Conclusions

The mechanical behaviour of sands and clays subject to normal (plastic) compression are very similar, albeit at different stress levels, despite the differences in inter-particle interactions (Hertzian normal

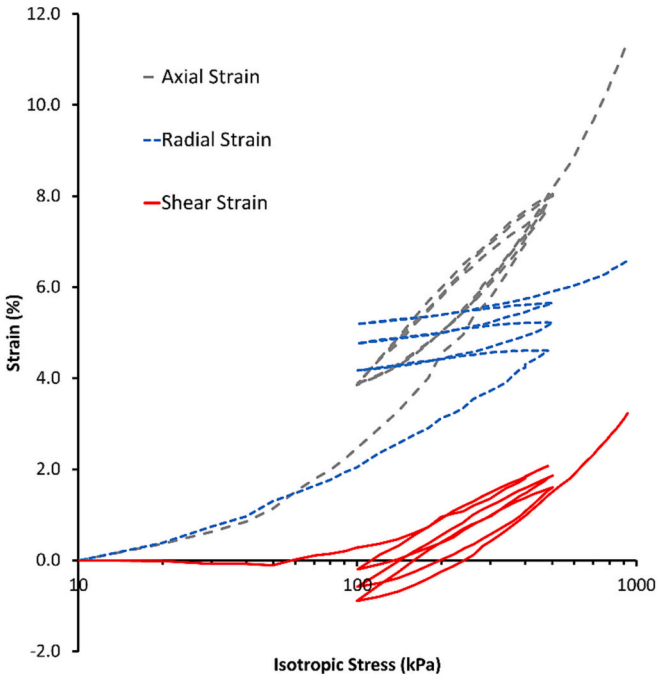

Fig. 6. Strains during compression.

contact forces or similar for sand) and electro-chemical forces for clays. Discrete element modelling (DEM) shows that the normal compression is related to "degradation" in some way in both cases. However, the unload-reload behaviour of sand and clay are not similar and clay exhibits hysteresis whereas sand does not. The purpose of this short paper has therefore been to shed light on the hysteretic clay behaviour at a particle scale. This paper has shown that the hysteresis is due to new edge contacts forming as radial strain "ratchets" under increasing cycles of load and this explains the volumetric compaction under cyclic loading in the absence of any well-defined "fracture" of stacks.

CRediT authorship contribution statement

John de Bono: Methodology, Investigation, Formal analysis, Writing – original draft. **Glenn McDowell:** Writing – review & editing, Supervision, Project administration, Funding acquisition, Formal analysis.

Declaration of Competing Interest

The authors declare that they have no known competing financial interests or personal relationships that could have appeared to influence the work reported in this paper.

Data availability

Data will be made available on request.

Acknowledgements

This work was supported by the Engineering and Physical Sciences Research Council [grant number EP/S016228/1].

References

Alcantar, N., Israelachvili, J., Boles, J., 2003. Forces and ionic transport between mica surfaces: implications for pressure solution. Geochim. Cosmochim. Acta 67, 1289–1304. https://doi.org/10.1016/S0016-7037(02)01270-X.

Aminpour, P., Sjoblom, K.J., 2019. Multi-scale modelling of kaolinite triaxial behaviour. Géotechnique Lett. 9, 178–185. https://doi.org/10.1680/jgele.18.00194.

Bandera, S., O'Sullivan, C., Tangney, P., Angioletti-Uberti, S., 2021. Coarse-grained molecular dynamics simulations of clay compression. Comput. Geotech. 138, 104333 https://doi.org/10.1016/j.compgeo.2021.104333.

Burland, J.B., 1990. On the compressibility and shear strength of natural clays. Géotechnique 40, 329–378. https://doi.org/10.1680/geot.1990.40.3.329.

Cui, Y.J., Nguyen, X.P., Tang, A.M., Li, X.L., 2013. An insight into the unloading/reloading loops on the compression curve of natural stiff clays. Appl. Clay Sci. 83–84, 343–348. https://doi.org/10.1016/j.clay.2013.08.003.

de Bono, J.P., McDowell, G.R., 2017. Micro mechanics of drained and undrained shearing of compacted and overconsolidated crushable sand. Géotechnique 68, 1–15. https://doi.org/10.1680/jgeot.16.P.318.

de Bono, J.P., McDowell, G.R., 2022a. Discrete element modelling of normal compression of clay. J. Mech. Phys. Solids 162, 104847. https://doi.org/10.1016/j.jmps.2022.104847.

de Bono, J.P., McDowell, G.R., 2022b. Some important aspects of modelling clay platelet interactions using DEM. Powder Technol. 398, 117056 https://doi.org/10.1016/j.powtec.2021.117056.

de Bono, J.P., McDowell, G., 2023a. Particle-scale simulations of the compression and shearing of kaolin clay. Géotechnique 1–40. https://doi.org/10.1680/jgeot.22.00423.

de Bono, J.P., McDowell, G.R., 2023b. Simulating multifaceted interactions between kaolinite platelets. Powder Technol. 413, 118062 https://doi.org/10.1016/j.powtec.2022.118062.

Gupta, V., Miller, J.D., 2010. Surface force measurements at the basal planes of ordered kaolinite particles. J. Colloid Interface Sci. 344, 362–371. https://doi.org/10.1016/j.jcis.2010.01.012.

Gupta, V., Hampton, M.A., Stokes, J.R., Nguyen, A.V., Miller, J.D., 2011. Particle interactions in kaolinite suspensions and corresponding aggregate structures. J. Colloid Interface Sci. 359, 95–103. https://doi.org/10.1016/j.jcis.2011.03.043.

Homola, A.M., Israelachvili, J.N., Gee, M.L., McGuiggan, P.M., 1989. Measurements of and relation between the adhesion and friction of two surfaces separated by molecularly thin liquid films. J. Tribol. 111, 675–682. https://doi.org/10.1115/1.3261994.

Homola, A.M., Israelachvili, J.N., McGuiggan, P.M., Gee, M.L., 1990. Fundamental experimental studies in tribology: the transition from "interfacial" friction of undamaged molecularly smooth surfaces to "normal" friction with wear. Wear 136, 65–83. https://doi.org/10.1016/0043-1648(90)90072-I.

Israelachvili, J.N., 2011. Intermolecular and Surface Forces, Third. ed. Academic Press. https://doi.org/10.1016/C2011-0-05119-0.

Kawai, K., Sakuma, H., Katayama, I., Tamura, K., 2015. Frictional characteristics of single and polycrystalline muscovite and influence of fluid chemistry. J. Geophys. Res. Solid Earth 120, 6209–6218. https://doi.org/10.1002/2015JB012286.

Kumar, N., Andersson, M.P., Van Den Ende, D., Mugele, F., Siretanu, I., 2017. Probing the surface charge on the basal planes of Kaolinite particles with high-resolution atomic force microscopy. Langmuir 33, 14226–14237. https://doi.org/10.1021/acs.langmuir.7b03153.

Liu, J., Miller, J.D., Yin, X., Gupta, V., Wang, X., 2014a. Influence of ionic strength on the surface charge and interaction of layered silicate particles. J. Colloid Interface Sci. 432, 270–277. https://doi.org/10.1016/j.jcis.2014.06.028.

Liu, J., Sandaklie-Nikolova, L., Wang, X., Miller, J.D., 2014b. Surface force measurements at kaolinite edge surfaces using atomic force microscopy. J. Colloid Interface Sci. 420, 35–40. https://doi.org/10.1016/j.jcis.2013.12.053.

Mitchell, J.K., Soga, K., 2005. Fundamentals of Soil Behavior, 3rd ed. John Wiley and Sons, Hoboken, New Jersey.

Pagano, A.G., Magnanimo, V., Weinhart, T., Tarantino, A., 2020. Exploring the micromechanics of non-active clays by way of virtual DEM experiments. Géotechnique 70, 303–316. https://doi.org/10.1680/jgeot.18.P.060.

Pedrotti, M., Tarantino, A., 2017. An experimental investigation into the micromechanics of non-active clays. Géotechnique 1–18. https://doi.org/10.1680/jgeot.16.P.245.

Sjoblom, K.J., 2016. Coarse-grained molecular dynamics approach to simulating clay behavior. J. Geotech. Geoenviron. Eng. 142, 1–6. https://doi.org/10.1061/(ASCE)GT.1943-5606.0001394.

Veeramasuneni, S., Yalamanchili, M.R., Miller, J.D., 1996. Measurement of interaction forces between silica and α-alumina by atomic force microscopy. J. Colloid Interface Sci. 184, 594–600. https://doi.org/10.1006/jcis.1996.0656.

Vigil, G., Xu, Z., Steinberg, S., Israelachvili, J., 1994. Interactions of silica surfaces. J. Colloid Interface Sci. 165, 367–385. https://doi.org/10.1006/jcis.1994.1242.

Wang, Y.-H., Siu, W.-K., 2006. Structure characteristics and mechanical properties of kaolinite soils. I. Surface charges and structural characterizations. Can. Geotech. J. 43, 587–600. https://doi.org/10.1139/t06-026.

Wood, D.M., 1990. Soil Behaviour and Critical State Soil Mechanics. Cambridge University Press.